Electrochemistry

The Electrochemical Society of Japan

Received: April 10, 2016
Accepted: May 10, 2016
Published: October 5, 2016

http://dx.doi.org/10.5796/electrochemistry.84.766

Communication Electrochemistry, **84(10)**, 766–768 (2016)

Catalytic Activities of Pt–Metal Alloys on Oxygen Reduction Reaction in Fluorohydrogenate Ionic Liquid

Pisit KIATKITTIKUL,[a,†] Jumpei YAMAGUCHI,[a,‡] Toshiyuki NOHIRA,[b,*] and Rika HAGIWARA[a]

[a] *Department of Fundamental Energy Science, Graduate School of Energy Science, Kyoto University, Sakyo-ku, Kyoto 606-8501, Japan*

[b] *Advanced Energy Utilization Division, Institute of Advanced Energy, Kyoto University, Uji, Kyoto 611-0011, Japan*

* *Corresponding author: nohira.toshiyuki.8r@kyoto-u.ac.jp*

ABSTRACT

Oxygen reduction reaction (ORR) rate constants (k) on Pt and Pt–M (M = Fe, Co, Ni) electrodes were evaluated in *N*-ethyl-*N*-methylpyrrolidinium fluorohydrogenate (EMPyr$(FH)_{1.7}F$) ionic liquid at 298–333 K. The Pt–Fe electrode exhibited the best catalytic activity in EMPyr$(FH)_{1.7}F$, because of the large surface area of its nanoporous structure after Fe dissolution. X-ray photoelectron spectroscopy and field-emission scanning electron microscopy showed that Co and Ni barely dissolved in EMPyr$(FH)_{1.7}F$. The observed ORR activities of Pt–Co and Pt–Ni alloys were lower than that of Pt in EMPyr$(FH)_{1.7}F$.

Keywords : Fluorohydrogenate Ionic Liquid, Oxygen Reduction Reaction, Pt Alloy, Fuel Cell

1. Introduction

In recent decades, ionic liquids (ILs) have received increasing attention as potential electrolytes for applications in electrochemical devices, because of their high chemical and thermal stabilities, nonflammabilities, nonvolatile natures, and wide electrochemical windows.[1–3] Our group has focused on fluorohydrogenate ILs (FHILs), which consist of organic cations and fluorohydrogenate anions, $(FH)_nF^-$, where n represents the average number of HF ligands attached to the fluoride anion. One of the firstly developed FHILs, 1-ethyl-3-methylimidazolium fluorohydrogenate (EMIm-$(FH)_{2.3}F$), exhibits high conductivity (100 mS cm^{-1} at 298 K), low melting point (208 K) and low glass-transition temperature (148 K),[4,5] making it a promising electrolyte for electrochemical devices.

We have already proposed operating mechanisms for non-humidified fuel cells using FHILs as electrolytes, which we called fluorohydrogenate fuel cells (FHFCs).[6] This type of fuel cell can be operated at high temperatures under nonhumidified conditions, because of their unique mechanism, which involves the transfer of hydrogen and charges by fluorohydrogenate anions. We also reported a nonhumidified fuel cell based on a composite membrane consisting of EMIm$(FH)_nF$ ($n = 1.3$ and 2.3) and poly(vinylidene fluoride-*co*-hexafluoropropylene).[7] However, in our later studies, *N*-ethyl-*N*-methylpyrrolidinium fluorohydrogenate (EMPyr$(FH)_{1.7}F$) was found to exhibit a higher activity toward the oxygen reduction reaction (ORR) on Pt electrodes and give a lower H_2O_2 yield than other FHILs,[8,9] making it a more promising electrolyte for nonhumidified fuel cells. A single cell using this FHIL had a higher maximum power density than that of the first reported FHFC.[10]

For FHFCs, as in the case of conventional PEFCs, Pt is generally used as the cathode catalyst. However, Pt is expensive, because of its scarcity (ca. 0.037 ppm in the Earth's crust[11]). The development of cathode catalysts containing smaller amount of Pt is therefore crucial. Various potential cathode catalysts such as Pt–M (M = Fe, Co, Ni, etc.) alloy catalysts,[12–23] Pt core–shell catalysts,[24,25] and Pt-free catalysts[26,27] have been investigated by many research groups. Among these, Pt alloy catalysts were found to exhibit better ORR activities than Pt in acidic solutions. Although much effort has been made to improve understanding of the ORR behavior of Pt alloys in acids,[28–30] there has been no report of detailed ORR behavior in FHILs. The ORR at an FHFC involves fluorohydrogenate anions rather than protons, therefore the ORR mechanism in FHILs may differ from that in conventional proton-conductive electrolytes, i.e., there may be catalysts that are uniquely effective for FHFC cathodes. It is therefore interesting to investigate the ORR activities of Pt alloys in FHILs.

In this study, Pt–Fe, Pt–Co, and Pt–Ni were selected as the Pt alloys, because they have been reported to have better specific activities than Pt in aqueous acidic solutions.[17,19,20] EMPyr$(FH)_{1.7}F$ was used as the electrolyte. The Pt alloys were prepared by sputtering deposition. The Pt:M (M = Fe, Co, Ne) ratios were determined using X-ray photoelectron spectroscopy (XPS). The ORR rate constants for the Pt alloys were compared with those for Pt in EMPyr$(FH)_{1.7}F$ at 298–333 K.

2. Experimental

Pt alloys were prepared using a radio-frequency magnetron sputtering deposition system (SVC-700 RF 2, Sanyu). A Pt disk substrate (diameter 5 mm, thickness 5 mm) was polished with emery papers and a buffing compound. The chamber was first evacuated to 1.0×10^{-3} Pa, and then Ar gas (Kyoto Teisan, >99.999%) was introduced up to a pressure of 5 Pa. The substrate surface was first etched using an Ar ion plasma for 30 min at room temperature to remove the surface oxide layer. A Pt, Pt–Fe, Pt–Co, or Pt–Ni layer was deposited by sputtering deposition, using Pt, PtFe, PtCo, or PtNi targets (Furuya Metal, purity 3 N), respectively, for 20 min at 573 K.

XPS was performed using a JPS-9010 MC instrument (JEOL) with Mg Kα radiation. Samples were fixed on carbon sheets. Before the measurements, the samples were etched for 20 s. The obtained peaks were corrected using the C1s peak at 248.6 eV.

[†]Present Address: Asahi Intecc, Nagoya, Aichi 463-0024, Japan
[‡]Present Address: Toray Industries, Chuo-ku, Tokyo 103-8666, Japan

A rotating disk electrode (RDE) assembly (Pine Research Instrumentation) was used to estimate the activities of the Pt and Pt alloys. Pt and Pt alloy disks were used as the working electrodes, and a Pt wire was used as the counter electrode. The reference electrode was a reversible hydrogen electrode (RHE) made of Pt wire and Pt black, which was inserted in the cell using a Luggin capillary. Electrochemical measurements were conducted using a potentio/galvanostat (IviumStat, Ivium Technologies). Dry hydrogen (purity >99.999%) was supplied from a hydrogen generator (HORIBA STEC) at a flow rate of 10 mL min^{-1}, and dry oxygen (Kyoto Teisan, >99.999%,) was supplied from a cylinder at the same flow rate. Prior to the electrochemical measurements, oxygen was bubbled into the cell for 2 h to saturate the electrolyte.

Surface images of the Pt alloys were obtained using field emission scanning electron microscope (FE-SEM, SU-8020, Hitachi).

3. Results and Discussion

Figure 1 shows the $Pt4f_{7/2}$ and $Pt4f_{5/2}$ XPS spectra for Pt, Pt–Fe, Pt–Co, and Pt–Ni. The solid curves represent the XPS spectra before the electrochemical measurements. The compositions of the Pt alloys were calculated from the peak areas to be $Pt_{55}Fe_{45}$, $Pt_{50}Co_{50}$, and $Pt_{50}Ni_{50}$. For all samples, the $Pt4f_{7/2}$ and $Pt4f_{5/2}$ peaks shifted slightly to higher binding energies with respect to pure Pt, which indicates alloy formation. It has been reported that the chemical properties of Pt are strongly related to the average energy of the d valence bands.[24] Electron transfer from nonprecious metals to Pt has been reported to induce rehybridization of the d band, resulting in a positive shift of the Pt4f core levels.[22–24] The results indicate that Pt–Fe, Pt–Co, and Pt–Ni alloys were successfully formed.

The ORR activities of the Pt alloys in $EMPyr(FH)_{1.7}F$ were evaluated by measuring the kinetically limited current density (j_k) using RDE method. The ORR rate constants (k) were calculated using the following equation:

$$j_k = nFkC \quad (1)$$

where F and C are Faraday constant and solubility of oxygen (0.58 mmol dm^{-3} for $EMPyr(FH)_{1.7}F$ at 298 K),[9] respectively. The values of n for Pt and Pt alloys are assumed to be 4.

Figure 2 shows Arrhenius plots of the rate constants for the ORR on the Pt, Pt–Fe, Pt–Co, and Pt–Ni electrodes in $EMPyr(FH)_{1.7}F$ at 298–333 K. In this temperature range, the ORR activity of Pt–Fe is higher than that of Pt. For example, the rate constant for the Pt–Fe

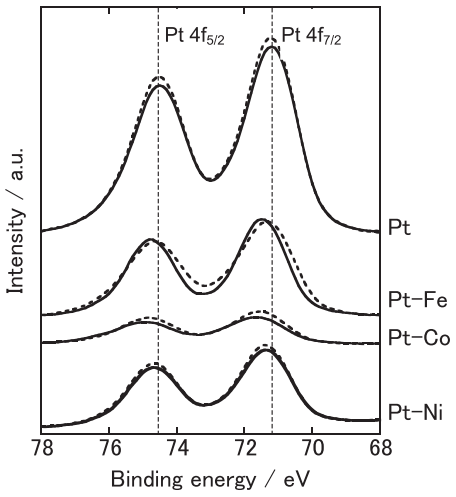

Figure 1. $Pt4f_{7/2}$ and $Pt4f_{5/2}$ XPS spectra of Pt, Pt–Fe, Pt–Co, and Pt–Ni before (solid curves) and after (broken curves) electrochemical measurements in $EMPyr(FH)_{1.7}F$ at 298–333 K. Dotted vertical lines indicate peak energies of $Pt4f_{7/2}$ and $Pt4f_{5/2}$ for Pt.

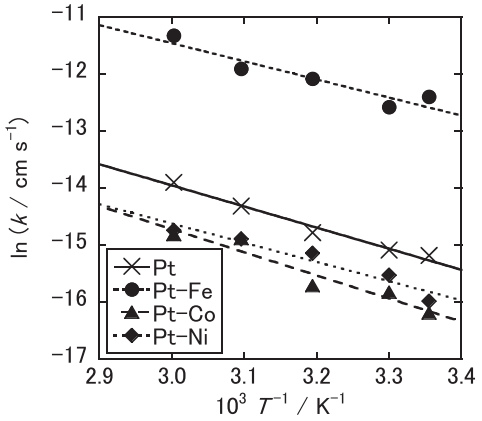

Figure 2. Arrhenius plots of ORR rate constants on Pt (×), Pt–Fe (●), Pt–Co (▲), and Pt–Ni (◆) in $EMPyr(FH)_{1.7}F$ at 298–333 K; $E = 0.9$ V vs. RHE.

electrode is 4.1×10^{-6} cm s^{-1} at 298 K, which is 16 times larger than that for the Pt electrode (2.5×10^{-7} cm s^{-1}) at 298 K. Higher ORR activities for Pt–Fe alloy electrodes have also been reported for aqueous acidic systems.[17,19,20] In contrast, in the present study, the Pt–Co and Pt–Ni alloys exhibited slightly lower ORR activities (8.8×10^{-8} and 1.1×10^{-7} cm s^{-1}, respectively, at 298 K) than that for Pt.

The activation energies of the ORR on Pt, Pt–Fe, Pt–Co, and Pt–Ni were estimated from the Arrhenius plots to be 30.8, 26.4, 33.6, and 28.0 kJ mol^{-1}, respectively. The activation energies on Pt and the Pt alloys were almost the same, suggesting the same reaction mechanism. In the cases of acidic media, the Damjanovic mechanism is widely accepted for the ORR on Pt.[28–30] According to this mechanism, the following oxygen electrochemsorption step is the rate-determining step:

$$O_2 + Pt + H^+ + e^- = Pt\text{-}O_2H_{ads} \quad (2)$$

Although the activation energies estimated in the present study are a little different from those reported in a previous study of Pt, Pt–Fe, Pt–Co, and Pt–Ni in in 0.1 M $HClO_4$ (ca. 40 kJ mol^{-1}),[17] the similar oxygen electrochemisorption step might be the rate-determining step in FHILs:

$$O_2 + Pt + 2[(FH)_2F]^- + e^- = Pt\text{-}O_2H_{ads} + 3[FHF]^- \quad (3)$$

The difference between H^+ and $[(FH)_2F]^-$ as the proton source might affect the activation energy.

The compositions of the Pt alloys after the electrochemical measurements were calculated from the peak areas of the XPS spectra. The broken curves in Fig. 1 show the $Pt4f_{7/2}$ and $Pt4f_{5/2}$ XPS spectra for Pt, Pt–Fe, Pt–Co, and Pt–Ni after the electrochemical measurements. The Fe, Co, and Ni contents decreased, giving the compositions $Pt_{91}Fe_9$, $Pt_{60}Co_{40}$, and $Pt_{51}Ni_{49}$, i.e., most of the Fe in Pt–Fe and some of the Co in Pt–Co dissolved in the IL, whereas the Ni in Pt–Ni was retained during the electrochemical measurements. The Pt–Fe composition is almost unchanged even after Ar ion bombardment, therefore Fe is lost even from the bulk of the sample. As expected from the Pt-rich composition, Pt4f peak shifts were not observed for the Pt–Fe alloy after the electrochemical measurements. These results indicate that the high ORR activity of Pt–Fe is not attributable to the nature of the alloy itself but is caused by the higher Pt surface area, which results from Fe leaching out of the alloy. Stonehart et al. reported that in the case of phosphoric acid fuel cells, similar phenomena were observed for a series of alloy systems such as Pt–V, Pt–Cr, Pt–Co, and Pt–Cu.[16]

The surface structures of the electrodes before and after the electrochemical measurements were observed using FE-SEM.

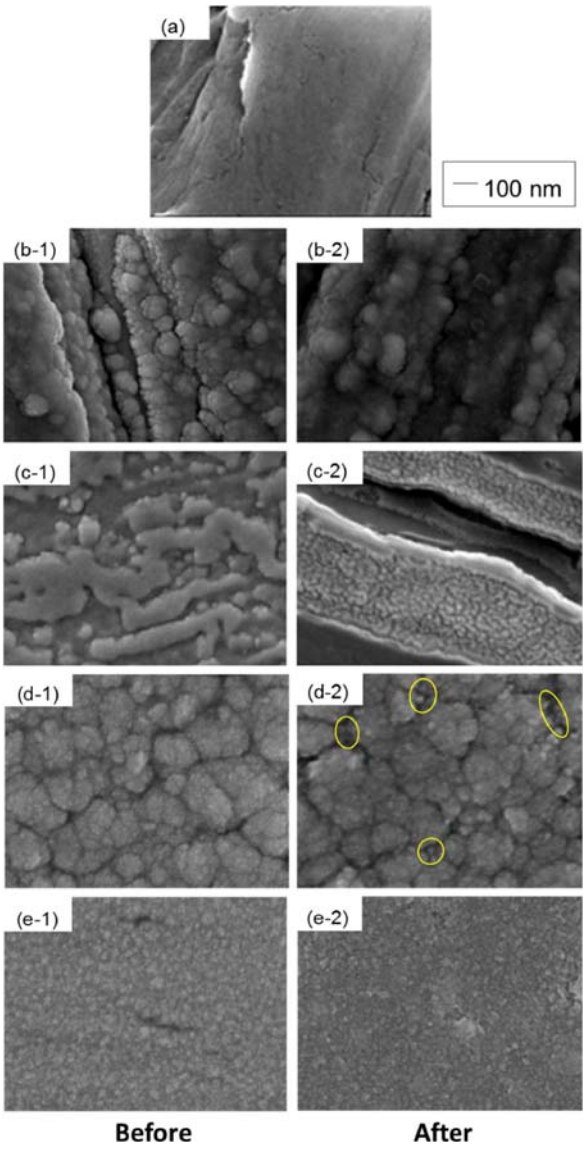

Figure 3. (Color online) FE-SEM images of (a) pristine Pt substrate, and (b-1, b-2) Pt-coated, (c-1, c-2) $Pt_{55}Fe_{45}$-coated, (d-1, d-2) $Pt_{50}Co_{50}$-coated, and (e-1, e-2) $Pt_{50}Ni_{50}$-coated Pt electrodes before and after electrochemical measurements in $EMPyr(FH)_{1.7}F$ at 298–333 K.

Figure 3(a) shows an image of the pristine Pt substrate for reference. Figure 3(b-1) and (b-2) show images of the Pt-coated Pt electrode before and after the electrochemical measurements, respectively. A comparison of Fig. 3(b-1) and (b-2) shows that there was no obvious change in the surface structure after the electrochemical measurements. Figure 3(c-1) and (c-2) show images of the $Pt_{55}Fe_{45}$-coated Pt electrode before and after the electrochemical measurements, respectively. A nanoporous structure was observed for the Pt–Fe alloy after the electrochemical measurements, as shown in Fig. 3(c-2). These results further support the suggestion that the enhancement of the ORR activity was caused by the rougher surface resulting from leaching of Fe from the alloy. To confirm this, however, more precise analysis of the surface area is necessary, which is our future task. Figure 3(d-1) and (d-2) show images of the $Pt_{50}Co_{50}$-coated Pt electrode before and after the electrochemical measurements, respectively. In Fig. 3(d-2), although a partial nanoporous Pt structure is observed (indicated with yellow circles), most of the surface is covered with a nonporous structure. The composition of $Pt_{60}Co_{40}$ determined by XPS after the electrochemical measurements is explained by the observation that the surface was mainly covered with the original $Pt_{50}Co_{50}$ and was only partly covered with nanoporous Pt. The ORR activity of the original $Pt_{50}Co_{50}$ was much lower than that of Pt, therefore the observed activity for the Pt–Co electrode was also lower than that for the Pt electrode. Figure 3(e-1) and (e-2) show images of the $Pt_{50}Ni_{50}$-coated Pt electrode before and after the electrochemical measurements, respectively. The morphology did not change significantly. This is consistent with the minimal change in the composition. Ni barely dissolved in $EMPyr(FH)_{1.7}F$, therefore the ORR activity was mainly attributable to the Pt–Ni alloy, and was lower than the ORR activity of Pt in $EMPyr(FH)_{1.7}F$.

4. Conclusion

The Pt–Fe electrode showed the highest ORR catalytic activity in $EMPyr(FH)_{1.7}F$ at 298–333 K. In contrast, ORR activities of Pt–Co and Pt–Ni electrodes were lower than that of Pt electrode. The activation energies of the ORR on Pt, Pt–Fe, Pt–Co, and Pt–Ni were estimated to be 30.8, 26.4, 33.6, and 28.0 kJ mol^{-1}, respectively. The high activity for Pt–Fe electrode is considered to be mainly due to the large surface area of nanoporous structure induced by dissolution of Fe. In contrast, the observed ORR activities for Pt–Co and Pt–Ni electrodes are mainly attributed to the alloys because Co and Ni barely dissolved into the FHIL.

References

1. K. R. Seddon, *J. Chem. Technol. Biotechnol.*, **68**, 351 (1997).
2. T. Welton, *Chem. Rev.*, **99**, 2071 (1999).
3. P. Wasserscheid and W. Kein, *Angew. Chem., Int. Ed.*, **39**, 3772 (2000).
4. R. Hagiwara, T. Hirashige, T. Tsuda, and Y. Ito, *J. Fluorine Chem.*, **99**, 1 (1999).
5. K. Matsumoto, R. Hagiwara, and Y. Ito, *Electrochem. Solid-State Lett.*, **7**, E41 (2004).
6. R. Hagiwara, T. Nohira, K. Matsumoto, and Y. Tamba, *J. Electrochem. Solid-State Lett.*, **8**, A231 (2005).
7. J. S. Lee, T. Nohira, and R. Hagiwara, *J. Power Sources*, **171**, 535 (2007).
8. Y. Tani, T. Nohira, T. Enomoto, K. Matsumoto, and R. Hagiwara, *J. Electrochim. Acta*, **56**, 3852 (2011).
9. P. Kiatkittikul, J. Yamaguchi, R. Taniki, K. Matsumoto, T. Nohira, and R. Hagiwara, *J. Power Sources*, **266**, 193 (2014).
10. P. Kiatkittikul, T. Nohira, and R. Hagiwara, *J. Power Sources*, **220**, 10 (2012).
11. M. Winter, *Abundance in Earth's crust: periodicity*, can be found under http://www.webelements.com/periodicity/abundance_crust/, (2015).
12. S. Mukerjee and S. Srinivasan, *J. Electroanal. Chem.*, **357**, 201 (1993).
13. E. Antolini, J. R. C. Salgado, M. J. Giz, and E. R. Gonzalez, *Int. J. Hydrogen Energy*, **30**, 1213 (2005).
14. J. T. Glass and G. L. Cahen, Jr., *J. Electrochem. Soc.*, **135**, 1650 (1988).
15. M. T. Paffett, J. G. Beery, and S. Gottesfeld, *J. Electrochem. Soc.*, **135**, 1431 (1988).
16. P. Stonehart and B. Bunsenges, *Phys. Chem.*, **94**, 913 (1990).
17. N. Wakabayashi, M. Takeichi, H. Uchida, and M. Watanabe, *J. Phys. Chem. B*, **109**, 5836 (2005).
18. V. Stamenkovic, B. S. Mun, K. J. J. Mayrhofer, P. N. Ross, N. M. Markovic, J. Rossmeisl, J. Greeley, and J. K. Nørskov, *Angew. Chem., Int. Ed.*, **45**, 2897 (2006).
19. H. Uchida, H. Yano, M. Wakisaka, and M. Watanabe, *Electrochemistry*, **79**, 303 (2011).
20. M. Watanabe, D. A. Tryk, M. Wakisaka, H. Yano, and H. Uchida, *Electrochim. Acta*, **84**, 187 (2012).
21. B. P. Vinayan, R. Nagar, N. Rajalakshmi, and S. Ramaprabhu, *Adv. Funct. Mater.*, **22**, 3519 (2012).
22. S. Mukerjee, S. Srinivasan, and M. P. Soriaga, *J. Phys. Chem.*, **99**, 4577 (1995).
23. S. Mukerjee, S. Srinivasan, M. P. Soriaga, and J. McBreen, *J. Electrochem. Soc.*, **142**, 1409 (1995).
24. M. Lefevre, E. Proietti, F. Jaouen, and J. Dodelet, *Science*, **324**, 71 (2009).
25. J. Ozaki, S. Tanifuji, A. Furuichi, and K. Yabutsuka, *Electrochim. Acta*, **55**, 1864 (2010).
26. M. Neergat and R. Rahul, *J. Electrochem. Soc.*, **159**, F234 (2012).
27. R. Lin, C. Cao, T. Zhao, Z. Huang, B. Li, A. Wieckowski, and J. Ma, *J. Power Sources*, **223**, 190 (2013).
28. A. Damjanovic and V. Brusic, *Electrochim. Acta*, **12**, 615 (1967).
29. D. B. Sepa, V. Vojnovic, and A. Damjanovic, *Electrochim. Acta*, **26**, 781 (1981).
30. O. Antoine, Y. Bultel, and R. Durand, *J. Electroanal. Chem.*, **499**, 85 (2001).